

ORAP: Optimized Row Access Prefetching for Rowhammer-mitigated Memory

MacCoy Merrell*, Daniel Puckett*, Gino Chacon†, Jeffrey Stuecheli‡, Stavros Kalafatis*, Paul V. Gratz*

*Department of Electrical and Computer Engineering

Texas A&M University, College Station, TX, USA

{maccoy.merrell, dpuckett98, skalafatis-tamu, pgratz}@tamu.edu

ginoachacon@gmail.com jeff.stuecheli@arm.com

†AheadComputing

Beaverton, OR, USA

‡Arm

Austin, TX, USA

Abstract—Rowhammer is a well-studied DRAM phenomenon wherein multiple activations to a given row can cause bit flips in adjacent rows. Many mitigation techniques have also been introduced to address Rowhammer, with some support being already incorporated into the JEDEC DDR5 standard, specifically for per-row-activation-counter (PRAC) and refresh-management (RFM) systems. Mitigation schemes built on these mechanisms claim to have various levels of area, power, and performance overheads. To date the evaluation of existing mitigation schemes typically neglects the impact of other memory system components such as hardware prefetchers. Nearly all modern systems incorporate multiple levels of hardware prefetching and these can significantly improve processor performance through speculative cache population. While hiding memory latencies, these prefetchers induce higher numbers of downstream memory requests and increase DRAM activation rates. The performance overhead of Rowhammer mitigations are tied directly to memory access patterns, exposing both hardware prefetchers and Rowhammer mitigations to cross-interaction. As a result, we find that the performance improvement provided by prior-work hardware prefetchers is often severely impacted by typical Rowhammer mitigations. In effect, much of the benefit of speculative memory references from prefetching lies in accelerating and reordering DRAM references in ways that can trigger mitigations, incurring extra latency and significantly reducing the benefits of prefetching.

This work proposes the Optimized Row Access Prefetcher (ORAP), leveraging abundant last-level-cache (LLC) space to cache large portions of DRAM rowbuffer contents to reduce the need for future activations. Working alongside the state-of-the-art Berti prefetcher in the first level caches, ORAP reduces DRAM activation rates by 51.3% and achieves a 4.6% speedup over the state-of-the-art prefetcher configuration of Berti and SPP-PPF when prefetching in an RFM-mitigated memory system. Under PRAC mitigations, ORAP reduces energy overheads by 11.8%.

I. INTRODUCTION

Rowhammer is a DRAM hardware vulnerability first discovered by Kim et al. [29] and further characterized in subsequent works [23, 38, 39]. Early works focused on how this could be leveraged to carry out various attacks [21, 31, 63], while contemporary research focuses primarily on developing or bypassing hardware mitigations. Many mitigation techniques have been proposed [28, 45, 49, 50, 52, 64], with strategies like targeted-row-refresh (TRR) having been adopted for use in industry [9, 18]. The JEDEC DDR5 standard currently supports some of these mitigations by standardizing refresh-management (RFM) [19] commands and the use of per-

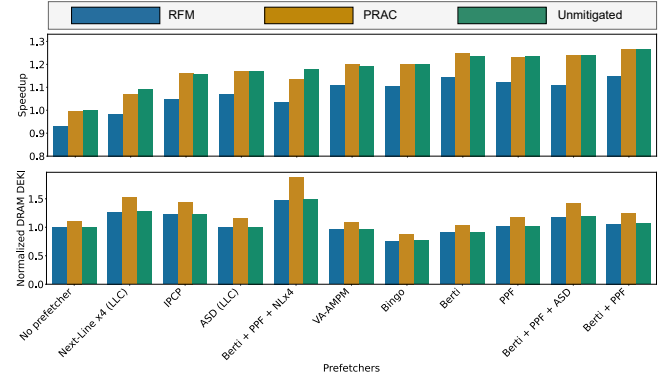


Fig. 1: Impact of Rowhammer mitigations on prefetcher single-core performance improvement (top) and DRAM dynamic energy per thousand instructions (bottom)

row-activation-counters (PRAC) [8, 20]. While these mitigation techniques broadly are able to reduce the likelihood of Rowhammer bit flips, this can come at some cost to performance and/or other overheads. Mitigation performance costs come in the form of higher DRAM latency and energy, particularly for memory-bound workloads.

Hardware prefetching is a well-studied and heavily utilized technique to improve performance [4, 6, 16, 37, 42, 44], where a prefetch engine within one of the CPU’s data caches learns and speculatively fetches cache lines that it believes will be used in the future. State-of-the-art prefetching systems display a 21.5% multi-core speedup over non-prefetching systems, a significant performance improvement for relatively little state.

Despite both Rowhammer mitigations and hardware prefetching being typically implemented in most commercial systems, generally the interactions between them have not been studied. Hardware prefetchers excel at reducing apparent memory latency, but are also known to induce additional memory requests over non-prefetching systems. The increased stress on the memory system is considered acceptable in academic works as the performance improvement is far more significant. Mitigation overheads, evaluated without these prefetchers, see an unrealistic system whose existing memory streams are well-ordered and efficient with heavy memory bot-

tlenecks. With prefetchers already included in nearly all shipping systems and Rowhammer mitigations seeing widespread adoption as systems are upgraded to DDR5 memories, these interactions are actively impacting real-world devices and are yet-to-be studied. Figure 1 shows the single-core geomean speedup of different prefetchers on Rowhammer mitigated systems alongside DRAM dynamic energy. We find that the speedup and energy costs of these policies are reliant on the mitigation used. In particular, RFM significantly reduces the performance benefit of prefetchers, while PRAC significantly increases their energy overhead.

In this work, we study the interactions of hardware prefetchers and Rowhammer mitigations. As described above, we find that in Rowhammer mitigated systems, prefetchers naturally induce more activations and hence trigger the mitigations more frequently, in turn inducing significant slowdowns and energy costs. To address this issue we propose the Optimized Row Access Prefetcher (ORAP), a last-level cache hardware prefetcher designed to reduce the negative interactions between the two systems, improving performance while lowering row activation counts. This work makes the following contributions:

- 1) We propose ORAP, a Rowhammer-mitigation- and DRAM-aware spatial data prefetcher within the LLC, designed to be used alongside other prefetchers in the L1 and L2 caches.
- 2) Unlike previous works in DRAM-aware prefetching, ORAP proactively avoids triggering DRAM activations through deep forward speculation and cache management. This is achieved without the addition of any new hardware in the memory controller or within the DRAM.
- 3) We develop a novel feedback technique for prefetching into large caches, prefetching with delayed usefulness information, and preventing excessive cache pollution.
- 4) ORAP increases the performance of RFM-based (that is, low-cost) Rowhammer-mitigated systems over the state-of-the-art by 4.6% without sacrificing security of the underlying RFM scheme and 3.3% for unmitigated systems. Under PRAC-based (high-cost) mitigations, DRAM dynamic energy is reduced by 11.8%.

II. BACKGROUND AND MOTIVATION

A. DRAM Organization

DRAM serves as main memory in nearly all modern computing. Capacitors paired with guard transistors store individual bits in large arrays. These capacitors lose charge over time, so rewrites (refreshes) are required to preserve memory integrity. Since system memory requirements vary, DRAM is typically populated within systems as needed, leading to wide variations in addressable space and available memory bandwidth. While appearing as a contiguous piece of memory to programmers, memory systems have subdivided DRAM into multiple levels to support these many different potential configurations. Figure 2 shows how these levels correlate to the physical devices. From within processors, memory controllers are duplicated per channel, each channel being operated independently and utilizing DDR protocols to transmit data on

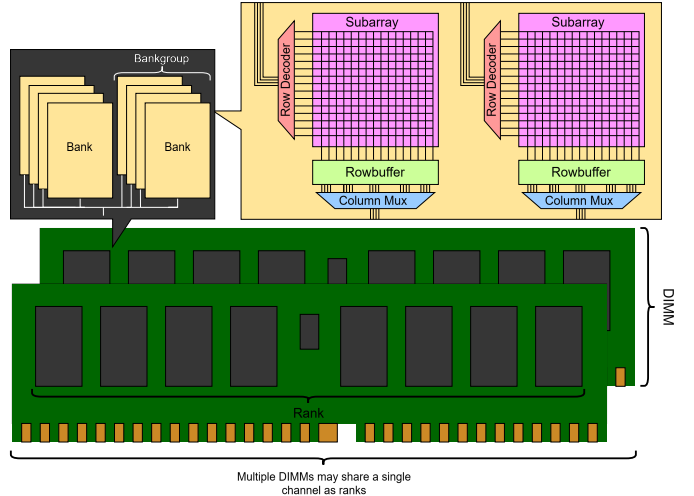


Fig. 2: The hierarchical organization of a dual in-line memory module (DIMM)

both clock edges. Within each channel, ranks of DRAM chips which form full words are addressed individually. Each of these ranks hosts dram banks which can operate in parallel, allowing multiple requests to be served simultaneously, though having to reserve a single channel shared with other ranks for the transmission of data. Each bank is addressed by a row and column address, which identifies which internal subarray is active and which bits of that subarray are read or written.

Reads and writes are issued at the bank level from/to the DRAM arrays. These operations are destructive and slow, so each bank instead acts upon entire rows at once, reading them into internal buffers called rowbuffers which can coalesce multiple DRAM operations before being written back to the array. While more complex than described here, activation commands (ACTs) to the DRAM serve as reads from the DRAM arrays into these rowbuffers, while precharge commands (PREs) serve as writes from these rowbuffers back into the arrays. Rowbuffers within a bank can only store a single row at a time, so it is far more performant to reaccess a rowbuffer with the target row than initiate a data transfer between the rowbuffer and array. Some mitigation schemes such as PRAC increase the time it takes to carry out PRE commands, which in turn can worsen energy consumption.

B. DRAM Address Mappings and Bank-level Parallelism

Balancing the cost of rowbuffer misses while maintaining maximum bank-level-parallelism (BLP) is a tradeoff managed by the memory controller and its address mappings. Logical-physical address mappings are designed by memory controller architects to offer the best performance to many different configurations by maximizing both BLP and rowbuffer hit rate simultaneously. To increase the chance of rowbuffer hits, some column addressing bits are kept low within the address space (referred to here-on as *column cluster bits*) while row addressing bits are kept high. The remaining placement of the bits for channels, banks, bankgroups, and ranks rely on

Row	Rank	Bankgroup	Bank	Channel	Column	Block Offset
35	20 19 18	17 16	14 13	12 11	6 5	0

(a) A naive address mapping that prioritizes rowbuffer hit rate

Row	Column	Rank	Bankgroup	Bank	Channel	Block Offset
35	20 19	14 13	12 11	10	8 7	6 5

(b) A naive address mapping that prioritizes bank parallelism

Row	Rank	Column	Bankgroup	Bank	Channel	Column	Channel	Block Offset
35	20 19	18 14	13 12	11 9	8	7	6	5

(c) Zen4 extrapolated from reverse-engineered mappings [18]

Fig. 3: 64 GiB DRAM logical-physical mappings

how memory architects have optimized their system. Placing these bits as low as possible like in Figure 3b maximizes the available BLP at the cost of bank access latency and rowbuffer hit rate, while placing these bits higher like in Figure 3a sacrifices BLP for instantaneous bank access latency and a higher rowbuffer hit rate.

The placement of these bank indexing bits varies between different processor manufacturers and technology generations, though they follow the general strategy of bisecting the column bits with the bank indexing [22], exploiting spatial locality for increased rowbuffer hits without disrupting available BLP. To further maximize BLP and avoid collisions, row bits are typically XORed with these bank index bits, resulting in different rows having different bank-wise strides. Recently, AMD’s Zen4 address mappings for their DDR5 memory controllers were reverse-engineered, showing that these techniques are still in use [18]. A mapping extrapolated from that work is shown in Figure 3c. For the remainder of this paper we will assume Zen4 mappings as they are the most recent known address mappings used in commercial products today.

Other works like Rubix [53] have suggested cryptographic-style address mappings to help disperse activations evenly throughout the memory, distributing column clusters across all rows in the DRAM. While this work reduces the number of activations that may accumulate on a single row, overall activation rates remain the same or are increased depending on which variation of Rubix is used.

C. Rowhammer

Rowhammer [30] is a well-studied attack vector in DRAM which exploits electrical disturbance effects in DDR memories to modify memory without direct access or privileges. These disturbance effects occur between DRAM rows within an array, allowing for operations upon one row to disturb nearby rows. Attackers induce high numbers of activations on aggressor rows to accumulate these disturbances and cause bit errors in nearby victim rows. The accumulated disturbance is limited only by the occasional rewrites from DRAM refresh or accesses to the victim row(s). Initially, in DDR3 technologies,

failures would require upwards of 100K nearby activations (referred to here as the Rowhammer threshold tRH), but as newer DDR4 technologies were introduced, this requirement dropped to as low as 4.8K activations [24]. Modern DDR5 technologies incorporate on-DRAM ECC and Rowhammer mitigations, making it difficult for the vulnerability of these new technologies to be assessed. With lowering tRH, the additional discovery of other potential disturbance mechanisms such as Rowpress [33], and varying levels of industry adoption, developing scalable low-overhead low-threshold mitigations has been an uphill battle.

1) *Academic Rowhammer Mitigations*: Many mitigation techniques have been proposed for Rowhammer [28, 40, 45, 49, 50, 52, 54]. Initially, probabilistic methods like PARA [30] were deemed sufficient, but as tRH decreased performance overheads were unsustainable. Many of these early mitigations were split between on-chip (in-memory-controller) and off-chip (in-DRAM) designs attempting to resolve this problem, some excluding the possibility of collaboration between processor and DRAM manufacturers. Various techniques were proposed, including denial-of-service [64], row migration [52], and tracking with selective refresh [28, 45, 49, 50]. In anticipation of further decreases in tRH, scalability has been the focus behind recent work, reducing overheads sufficiently such that they are bearable into the far future. With the onset of DDR5, new memory standards emerged, processor-DRAM cooperation was standardized, and the field of Rowhammer mitigations solidified.

2) *Rowhammer Mitigations in DDR5*: Support for two mitigation types have been added to the DDR5 JEDEC standard, refresh management (RFM) [19] and Per Row Activation Counting (PRAC) [8, 20]. Both of these components focus primarily on off-chip mitigation and are differentiated by the amount of state required for each and required design complexity. RFM, and RFM-based mitigations like MINT [28, 49], are considered low-cost as they require little additional state, while PRAC and PRAC-like mitigations [43, 50] require significant amounts of state in the form of counters in each DRAM row. As depicted in Figure 4a, the refresh management command in RFM allows the memory controller to reserve time for a vendor’s on-DRAM system to perform mitigation. Due to the proprietary nature of vendors’ mitigation schemes and internal DRAM array layouts, the memory controller blindly reserves time by issuing these commands after a certain number of DRAM ACT commands, regardless of the actual accumulated disturbances on DRAM rows or whether mitigations may be invoked. Per-row-activation counters (PRAC) work on a separate principle as seen in Figure 4b, with per-row counters in the DRAM allowing for exact tracking of how close rows are to tolerated thresholds. While PRAC prevents unnecessary mitigation from occurring (improving performance), the altered timings required to update the counters incur significant energy overheads. Multiple works explore how these techniques can be further improved, improving power and performance overheads or rectifying security flaws [9, 43, 47, 48, 60]. RFM systems insert timing bubbles at

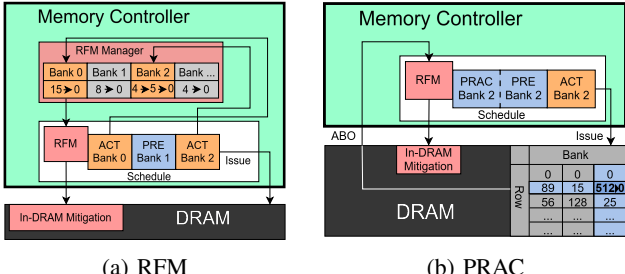


Fig. 4: RFM and PRAC Architecture

a rate correlated to the vendor’s defined RFM threshold and rate of activations in the DRAM. As a vendor’s defined RFM threshold becomes lower (which results in a lower tolerated tRH), or a workload induces a high ACT rate within the DRAM, RFM’s overheads become more costly. While PRAC’s mitigation costs can be hidden behind refresh (which can be insecure [48]), the significant overheads to PRE commands within the DRAM also cause slowdown, though reportedly less than seen in simulation [27] when using friendly memory controller row-policy. The exact performance overheads to each of these schemes are variable, depending on the workload and system configuration. Within our simulated system, PRAC (with a threshold of 512) and RFM (with a threshold of 16) had a 0.15% and 5.1% multi-core performance slowdown respectively. Both of these overheads are tied to ACT commands, either entirely as in the case of RFM or in part (PRE-ACT collisions in the memory controller) in the case of PRAC.

If the absolute number of DRAM activations are increased when running a given workload, it can be expected that the overhead (both in performance and energy) of whatever mitigation is in place would be significantly increased. If underlying policies or other mechanisms are introduced to decrease the number of DRAM activations, the expected overheads would be significantly reduced. Likewise, one would expect that techniques which can (in some cases dramatically) increase activations, such as hardware prefetching, would likely have an impact on overheads of these mitigation techniques. We note that, despite the large numbers of works in Rowhammer mitigations to date, we are aware of no prior work to examine the intersection of hardware prefetching and Rowhammer. Further, we are not aware of any existing mitigation works that discuss using prefetching in the baseline system setup of their experiments.

D. Hardware Prefetching

Hardware prefetchers speculatively fill CPU caches with timely and accurate data prior to their demand fetch. Simple prefetchers, such as shown in Figure 6, use a static pattern (fetching the next data block) while modern prefetchers attempt to identify and exploit complex access patterns.

Most recent advanced prefetchers identify spatial (address-based) patterns and then use those patterns to produce speculative future streams of accesses ahead of the current demand [6, 16, 25, 37, 42, 44]. Some spatial prefetchers [25],

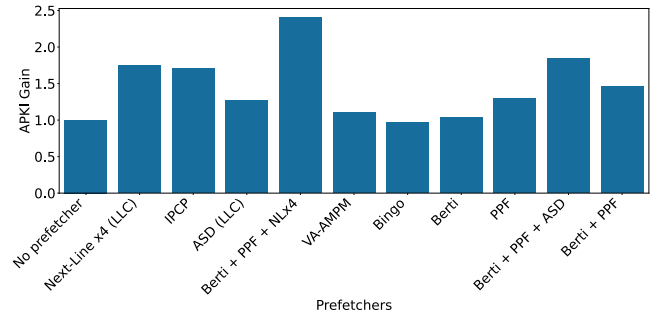


Fig. 5: Geomean increase in activations per thousand instructions (APKI) when adding prefetchers on single-core workloads.

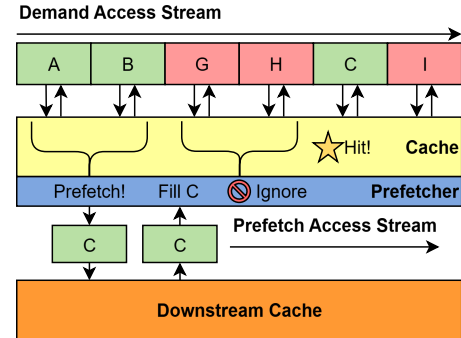


Fig. 6: A simple hardware prefetcher

are known to have been implemented in recent commercial processors [7, 12]. Some prefetchers such as Berti [42] also incorporate temporal data to further improve performance.

1) *Multi-level Hardware Prefetching*: While early prefetchers were typically designed in isolation, recent works examine prefetching in multiple cache-levels. Modern prefetchers, including Berti [42], PPF [6], and IPCP [44] each utilize some form of multi-level prefetching. Since prefetches from one level can trigger prefetches from another level, losses due to inaccuracy can become multiplicative and systemic misbehaviors of one prefetcher trigger misbehaviors in another. Likewise an LLC prefetcher, if it were added, would suffer from the compounded misbehaviors of all instances of hardware prefetchers within the system.

2) *Behaviors of Hardware Prefetchers*: As the amount of data pulled into caches by hardware prefetchers increases, so does the strain on the memory system. To understand why prefetchers induce additional memory strain, one must consider *why* prefetchers improve performance. Of the three types of cache misses, prefetchers excel in their ability to prevent both compulsory and capacity misses. The ability to issue prefetches ahead of time can bring in fresh data or large data sets before they invoke cache misses, and data can continue to be brought in until replacement policies force the eviction of data within the current access window. In this model, caches perform the role of a temporary buffer for future

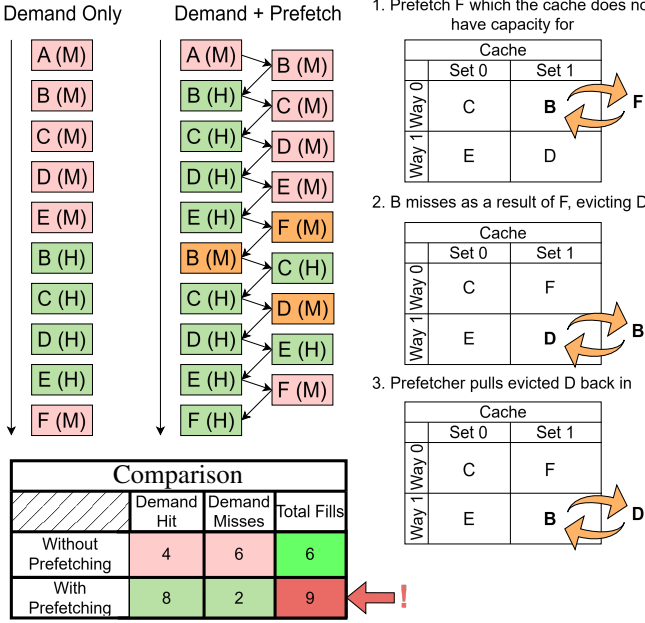


Fig. 7: A next-line prefetcher induces cache churning

data, rather than storage for frequently- or recently-used data. Avoiding a capacity miss involves bringing in useful data while also evicting useful data.

Figure 7 depicts a repeating streaming access pattern on a 4 entry LRU cache. Without prefetching, the stream has a low cache hit rate of 40%, but with a simple next-line prefetcher the hit rate can be raised up to 80%. However, this comes at substantial cost to the memory system. Blocks F, B, and D form an eviction chain that did not exist in the original non-prefetching system. These additional misses lead to a 33% increase in cache fills, though they come at no apparent performance loss. The net effect is improved performance, but *the cache is a cache in name only*, ultimately only serving as a buffer for prefetched data prior to its use. This is a problem for prefetchers which exist in systems where memory bandwidth is constrained as the increased memory access latency dominates over the cache hit rate improvement. This churning behavior spills over into lower levels of the memory hierarchy, increasing activation rates in the DRAM. This is not isolated to a single workload or prefetcher, as shown in Figure 5.

E. Co-aware Prefetcher and Memory Controller Policies

While no techniques we are aware of have examined Rowhammer mitigation in the context of a cache hierarchy with prefetching, some techniques have shown that cooperation between memory controllers and cache prefetchers can significantly increase rowbuffer hit rates. DA-AMPM [17] and the Open-Page Minimalist [22] scheduler both rely on batching prefetch requests to the same DRAM rowbuffer into bursts, preventing small request reorderings from inducing additional ACTs. These policies, which predate existing Rowhammer mitigations, focus on short-term, reactive, activation avoid-

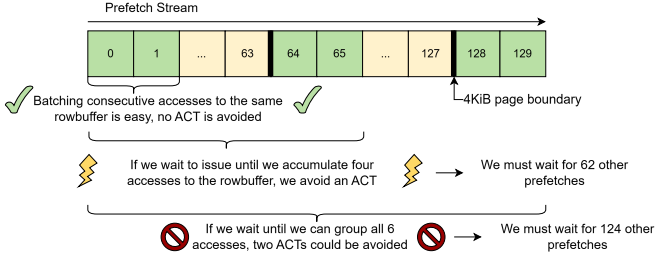


Fig. 8: Batching more than one column cluster is impossible for existing methods

ance. Only DRAM requests that exist within the system at the same time and going to the same place can be batched. This limits which activations can be avoided and fails to avoid ACTs to rowbuffers that may be avoidable but occur over longer timespans or are part of larger access patterns. Importantly, prefetch streams that cross over multiple column clusters cannot be batched retroactively. This represents a substantial number of activations that cannot be avoided. For address mappings like that used by the Zen4 system [18], this implies a pessimistic goal of 32 activations to pull in the entire rowbuffer’s content, under ideal operation. This is significantly more than the bare minimum of 1 activation that could be required, but presents challenges. As seen in Figure 8, larger addressable memory sizes have resulted in the spatial distance between consecutive column clusters increasing to the point where clusters within a rowbuffer are both spatially and temporally isolated. Waiting for these requests to coalesce to avoid an activation effectively abandons those prefetches, delaying them by thousands of cycles.

Another difficulty comes from page size restrictions; only a small number of cache lines are co-located within a single rowbuffer for standard 4 KiB page sizes. This results in the maximum batching size being limited to the number of column bits addressable within the page offset (a single column cluster). Page sizes are not fixed at 4 KiB, so systems which utilize larger page sizes can circumvent this final issue. Even if all these problems are ignored, banks must handle requests serially, resulting in long access times and potential denial of the bank to others if too many column clusters are fetched at once.

F. 2 MiB Pages in Modern Systems

Modern systems support several page sizes from KiBs to GiBs. Using large pages reduces translation overheads, while the drawbacks of larger page sizes can be avoided with proper operating system management [13]. OS kernels are very successful at automatically utilizing these page sizes, so programs do not need to explicitly allocate large pages [35, 36, 41]. Recent work has shown [51, 58] that most if not all pages in modern systems running current OSes are 2 MiB. Thus, unless otherwise specified, we assume 2 MiB pages for the remainder of this work.

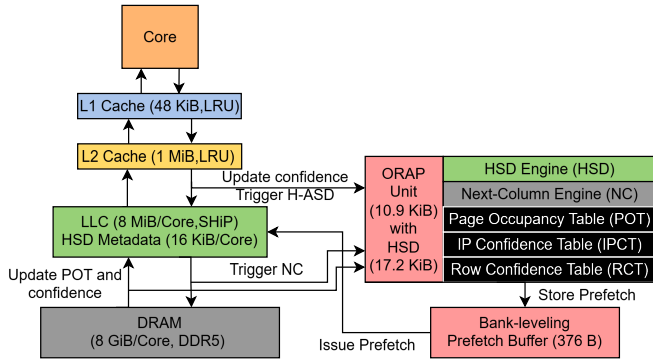


Fig. 9: ORAP Architecture

G. Summary

Prior work in co-aware prefetcher and memory controller designs are insufficient to exploit new technological advances and avoid performance drawbacks from Rowhammer mitigations in modern memory. Prefetcher designs have yet to adapt to recent changes in DRAM technologies, and, depending on the workload, may fail to meet the expected performance. Overcoming these obstacles is not trivial, and will require a targeted prefetcher design.

III. DESIGN

With consideration to the techniques, interactions, and obstacles described in Section II, we introduce the Optimized Row Access Prefetcher (ORAP).

A. Overview

Depicted in Figure 9, ORAP addresses the limitations of previous techniques via deep proactive prefetch streams. Instead of opportunistically reducing DRAM activations like DA-AMPM [17], ORAP’s primary goal is to actively avoid inducing activations. To achieve this, ORAP’s Next-Column prefetch engine exploits long access streams to DRAM. Triggered on a cache miss, ORAP utilizes its instruction-pointer-confidence-table (IPCT) and row-confidence-table (RCT) to assess the likelihood that ORAP will be able to successfully cache other data within the missing request’s target row. ORAP will then issue a variable number of prefetch requests, intending to piggy-back on the LLC miss to the DRAM and fetch additional information from the rowbuffer once it is opened. This results in large amounts of data being pulled into the LLC without additional activations. Under ideal circumstances, future DRAM activations are avoided and replaced with cache hits in the LLC.

A page-occupancy-table (POT) tracks the data recently brought into the cache to act as a filtering mechanism. To prevent the buildup of prefetch requests behind a DRAM bank, a bank-mapped prefetch buffer is maintained and managed (inspired by [32]). This queue serves to maximize BLP while also limiting the number of pending requests the prefetcher can have to a single bank.

Since Next-Column can only trigger on cache misses and targets a single bank, ORAP does not issue any mid-range

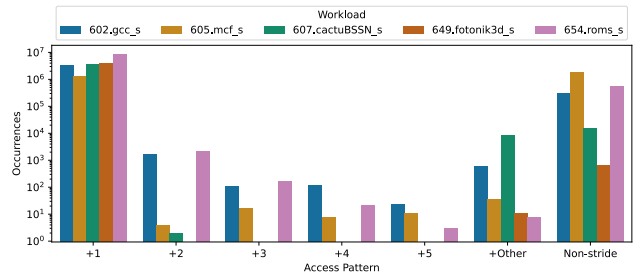


Fig. 10: Occurrences of stride access patterns from LLC misses in SPEC2017 workloads

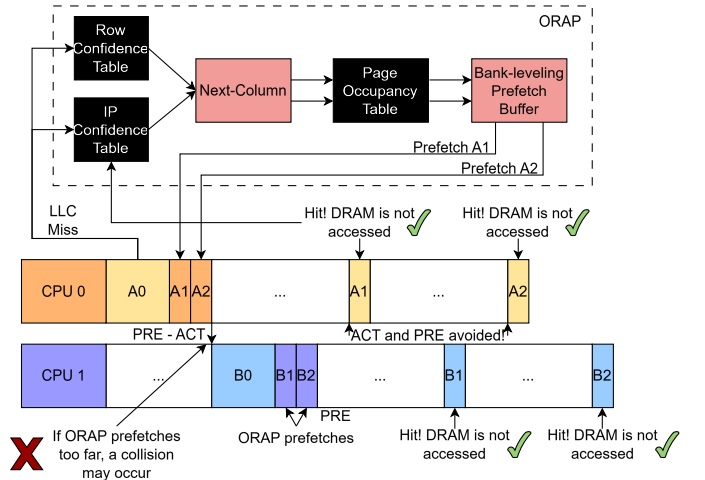


Fig. 11: ORAP prefetches across columns

prefetches by itself and does not exploit any bank parallelism. Therefore, the addition of a second prefetch engine to issue requests in a traditional fashion allows ORAP to have multiple banks serving Next-Column prefetches simultaneously. In this work, we utilize HSD (an ASD-inspired prefetcher [14] further discussed in Section III-E) to fulfill this role. For security purposes, ORAP’s internal state is duplicated per-core and no information is shared between cores.

Retaining many long-term prefetches in the LLC significantly disturbs the cache replacement policy. Some work has been done on integrating replacement policies with hardware prefetching [26, 62]. We evaluate ORAP under SHiP [61], a popular academic policy that utilizes the program counter (IP) and the reuse distance of cache accesses when making replacement decisions. We find that prefetching from within the LLC greatly disturbs the standard SHiP replacement policy, resulting in performance loss. To rectify this, SHiP in ORAP’s system ignores all prefetch accesses when collecting information or incrementing reuse counters. Unlike other works, this requires no additional state or logic in the SHiP policy.

B. Avoiding DRAM Activations

Typical prefetchers are incapable of avoiding DRAM activations that are the result of column cluster crossings. The distance between subsequent column clusters is upwards of 64

blocks, which is outside the typical range that even aggressive prefetchers will attempt. Instead of pulling in all cache lines between the current and future column clusters, ORAP prefetches only the next column clusters. This reduces the required total prefetches by 33x at the cost of an irregular stride pattern. Fortunately, LLC misses are heavily biased towards long, streaming access patterns as shown in Figure 10. This allows ORAP to use this irregular stride to pull in relevant data while retaining good usefulness.

As illustrated in Figure 11 ORAP’s Next-Column engine triggers only on cache misses. Depending on the confidence, ORAP will attempt to pull in a variable length of column clusters from the rowbuffer. Since ORAP issues prefetches on a cache miss, no additional activations are required to the target bank to serve these requests. Since these blocks now reside in the cache, future activations to access these column clusters are avoided. To prefetch within a single bank’s rowbuffer, ORAP must know the logical-physical mapping used by the memory controller. This incurs a one-time setup cost to inform the prefetcher when the system initializes, and therefore has negligible performance impact.

C. Confidence Challenges in Large Caches

Prefetchers must choose how aggressively to issue prefetches. Confidence is a measure of the ability of a given prefetcher to issue useful prefetches and can be used as the metric to dynamically determine the aggression of the prefetcher. Confidence can be tracked globally or locally by associating confidence with some feature of accesses into the cache. Features include IPs such as in Fu et al. [10] but can also be spatial access patterns as in SPP [25] or latency in the case of Berti [42]. Utilizing confidence from feedback mechanisms can be difficult in large caches. The feedback of whether a prefetch is useful or useless is temporally distant from when it was issued; the feedback is generally stale. Thus, the prefetcher throttles itself only after it has been behaving poorly for a long time. To account for this, ORAP treats confidence as a “pending prefetch counter”. Issuing a prefetch decrements the counter. Low confidence leads to few prefetches being issued before confidence drops to 0, while high confidence allows many prefetches to be issued before reaching 0. Confidence for a given IP and row is incremented once prefetches receive demand hits in the LLC. Confidence will slowly rise for prefetches whose usefulness allows a net gain in confidence, while slowly lower if usefulness falls below the necessary threshold.

D. Hybrid Confidence

ORAP tracks confidence based on both the address space (DRAM row) and origin instruction (IP). Tracking only IP or row fails to exploit workloads which demonstrate only strong IP- or address-based patterns. By allowing IPs with high confidence to prefetch data in low confidence rows and IPs with poor confidence to prefetch in high confidence rows the coverage of ORAP is increased.

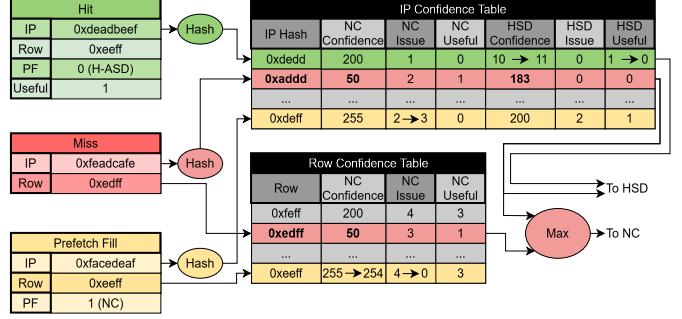


Fig. 12: Management of IPCT and RCT Tables for Cache Operations

The instruction-pointer-confidence-table (IPCT) and row-confidence-table (RCT) manage tracking IPs and rows using set-associative structures with LRU replacement. Each table is indexed by a 16-bit hash of the IP and row-id respectively. Since IP information for the original prefetch is not stored within the cache, cache hits resulting in a useful prefetch are attributed to the hitting IP, rather than the triggering IP of the prefetch. We find this sufficient since the IPCT is designed specifically for long single-IP streams which will likely be both the trigger and consumer of any prefetched data.

The confidence tables are updated on different types of cache accesses, and the exact updates made are summarized in Figure 12. For cache hits due to useful prefetches, the useful counter in the IPCT and RCT is incremented for the given row and IP, with only the IP used if the prefetch originated from HSD. On a prefetch fill, the IPCT and RCT increment their issue counter similarly to the useful counter. If either counter rolls over, the confidence stored within the table is incremented if it was the useful counter or decremented if it was the issue counter. When confidence is required (a cache miss for Next-Column or any cache access for HSD), the confidence from the tables (only the IPCT in the case of HSD, or both in the case of Next-Column) is provided to each engine.

Depicted in Table I, the values that the issue and useful counter maximums are set to impacts the target usefulness of ORAP. The issue counter maximum also provides absolute limits to the number of pending prefetches from a given IP or row that can reside in the cache without feedback (depending on how far the confidence is incremented). The potential range of pending prefetches are tabulated in Table II for different confidence increments and issue counter maximums. Limiting the total prefetches a row or IP can have pending in the cache prevents long feedback times from resulting in many useless prefetches. It also remains flexible, such that if feedback times are reduced confidence is allowed to rise quickly and the confidence is not unnecessarily throttled.

Once the confidence value is obtained for a row or IP, these are translated into different metrics for use by the relevant prefetch engine. In the case of Next-Column, the confidence will determine how many column clusters into the future ORAP will attempt to prefetch. Because prefetching even one

		Target Prefetch Usefulness					
		Useful Counter Max					
		1	2	3	4	5	6
Issue Counter Max	1	100%					
	2	50%	100%				
	3	33%	66.7%	100%			
	4	25%	50%	75%	100%		
	5	20%	40%	60%	80%	100%	
	6	16.7%	33.3%	50%	66.7%	83.3%	100%

TABLE I: ORAP’s targeted prefetch usefulness across different counter maximums.

		Maximum Pending Prefetches			
		Confidence Increment			
		1	2	3	4
Issue Counter Max	1	255	127	85	63
	2	510	255	170	127
	3	765	382	255	191
	4	1020	510	340	255
	5	1275	637	425	318
	6	1530	765	510	382

TABLE II: ORAP’s maximum pending prefetches across counter configurations.

column cluster into the future is risky, ORAP will selectively prefetch on only a fraction of low-confidence triggers (9.5% per 10 confidence, dropping no prefetches at 100 confidence). This also allows for triggers with 0 confidence to eventually be allowed to prefetch again, since they may slowly be allowed to issue prefetches and rebuild confidence.

A histogram probability is provided to HSD instead of a distance. This controls how deep HSD will prefetch, according to the probability of a stream reaching a certain depth. As confidence falls, the probability requirement increases and as confidence rises, the probability requirement falls.

E. HSD

ORAP’s Next-Column prefetcher by itself does not prefetch forward in the logical space and is thus limited to the bank the original LLC miss is on. This results in issues, as while ORAP can prefetch many blocks from a single bank, it cannot exploit any bank parallelism which limits the amount of DRAM bandwidth ORAP can utilize. We utilize a second prefetcher to learn LLC access patterns, predict future accesses, and cause cache misses to other banks that ORAP can then utilize.

ASD [14] is a prefetcher designed with similar goals in mind, however, ASD was originally proposed in an era of much smaller DRAM systems and thus does not leverage new advancements. Originally, ASD was proposed as a LLC-miss prefetcher, residing within the memory controller which would prefetch blocks into a reserved prefetch buffer. This technique fails to utilize the space available in the CPU caches, and is limited to the information available within the memory controller. Instead we propose a new prefetcher, Hybrid Stream Detection (HSD), inspired by ASD but designed to modern constraints. HSD utilizes ASD’s stream histogram technique to probabilistically issue prefetches in the logical space up to a depth of 64 blocks. Unlike traditional ASD, our HSD utilizes a hybrid IP and address technique similar to what is described

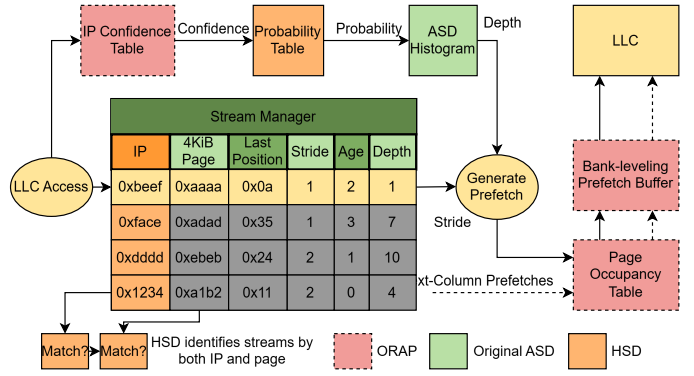


Fig. 13: HSD’s Architecture

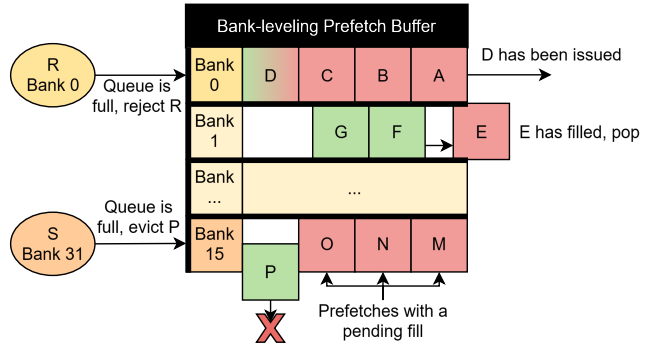


Fig. 14: Bank-leveling Buffer Architecture

in Section III-D to identify streams. Shown in Figure 13, streams are collated either by matching IP or if they fall within the same 4 KiB page which yields better performance than using either method alone. Additionally, instead of prefetching forward with a minimum probability of 50%, HSD utilizes the IPCT table to dynamically set the probability according to confidence. HSD’s prefetch engine triggers on all LLC accesses and its generated prefetches are first sent through the LLC before heading to DRAM. The column prefetch engine is therefore able to exploit HSD’s cache misses in the same way as the standard LLC misses. Running two prefetch engines within the same cache leads to many redundant prefetches being generated. To help synchronize information between ORAP’s internal prefetch engines, the page-occupancy-table (POT) is used to filter both engines.

F. Preserving Bank-level-parallelism

Issuing many prefetches to individual DRAM banks leads to undesirable impacts on DRAM bandwidth utilization. Consecutive requests to a single DRAM bank are required to wait serially to be served. If a demand request to the same bank arrives, it must either wait or the memory controller scheduler must preempt the previous prefetch requests, suffering two additional row activations but serving the critical demand request immediately. There are no additional benefits of issuing multiple requests simultaneously to the same DRAM bank from the LLC, and it only serves to occupy valuable MSHR space. Previous work [32] has tried to manage this through the

LLC's allocation of MSHRs and scheduling of its internal miss queue. This is difficult to implement for modern systems, as the number of DRAM banks on a single chip have scaled from 8 to 32. Considering that these banks are duplicated across DRAM ranks and channels, it is not feasible to have queues for each physical DRAM bank. Additionally, not all memory configurations will utilize the maximum number of DRAM banks, leaving significant amounts of hardware inactive.

Instead, pictured in Figure 14, we schedule prefetches according to DRAM bank as they leave ORAP rather than trying to reorder them as they miss in the cache. A set of bank-indexed buffers are shared between each instance of ORAP. As prefetches are generated, they are inserted into the buffer according to their destination bank ID. Unlike a standard queue, the prefetch buffer operates as an MSHR, holding buffer positions as occupied until prefetches return from issue or are dropped. If contention on a bank is high, the return time of prefetches to ORAP will throttle its requests to the bank due to the buffer filling. ORAP issues as many as two prefetches (one from two bank buffers) every cycle. To limit the amount of necessary hardware, the prefetch buffer is aliased into a smaller number of sub-buffers. This allows for efficient support for many different numbers of DRAM banks without excessive hardware requirements or large state left unused.

IV. EVALUATION

In this section, we evaluate ORAP against the current state-of-the-art hardware prefetcher configuration in single-core and 8-core simulations.

A. Methodology

We evaluate ORAP and other prefetchers within ChampSim, a micro-architectural trace-based simulator [11]. To ensure conformity with DDR5 standards, ramulator2 [34] is used as the DRAM model instead of ChampSim's internal model.

We use the SimPoint methodology [46] on traces from the SPEC2006, SPEC2017, GAP, and XSBench benchmark suites [5, 55–57]. For our single-core simulations traces are first run for 200M instructions before data collection, followed with data collection for 200M instructions. For 8-core simulations, the simulation is run until all 8-cores have executed 200M instructions, and then statistics are collected until they all have executed another 200M instructions. To support ORAP, ChampSim's page sizes are set to 2 MiB which is supported on most modern machines [1–3, 15, 35, 41].

We compare ORAP against various academic prefetchers in single-core simulations, including ASD, VA-AMPM, Bingo, Berti, IPCP, and SPP-PPF. In multi-core, ORAP is evaluated against the state-of-the-art configuration of Berti in the L1D and SPP-PPF in the L2C. We evaluate under both PRAC and RFM mitigations. The reverse-engineered mappings from AMD's Zen4 processor are used for DRAM mappings within the memory controller, as they represent the most-recent example of industry mappings [18]. For further accuracy,

Cache Configuration			
	Entries (Size)	Ways	Latency (cycles)
I-TLB	256	8	1
D-TLB	96	6	1
S-TLB	2048	16	7
L1I	32 KiB	8	4
L1D	48 KiB	12	5
L2	1 MiB	16	10
LLC	8 MiB/Core	16	60
MSHR Entries			

Core Configuration		Memory Controller Configuration	
Frequency	4 GHz	Channels	2 1-core, 4 8-core
Branch Predictor	Hashed Perceptron	Ranks	1 1-core, 2 8-core
Issue Width	6	Scheduler	Minimalist Open Page
Retire Width	8	Row Policy	Adaptive Row Policy
Scheduler Size	205	Address Mapping	Zen4 (8 GiB, 64 GiB)
ROB Size	512	RFM Threshold	16
LQ Size	192	PRAC Threshold	512
SQ Size	114	Blast Radius	2

DRAM Configuration		DRAM Timings	
	Standard	Standard	PRAC
Standard	DDR5		
MTPS	6400	16.25 ns	16.25 ns
Rows	65536	16.25 ns	16.25 ns
Columns	1024	16.25 ns	36.25 ns
Banks	4	32.5 ns	16.25 ns
Bankgroups	4 1-core, 8 8-core	nRC	48 ns
Density	16 GiB	nWR	30 ns
Channel Width	32-bit	nRTP	10 ns
Physical Size	8 GiB/Core		
Refresh Period	32 ms		

TABLE III: System Configuration

Structure	Breakdown	State
IP Confidence Table	1024 entries, 8 ways, 25 (38) bits per entry: 9-bit IP tag, 3-bit LRU, 8-bit confidence / engine, 3-bit issue counter (max 5) / engine, 2-bit useful counter (max 4) / engine	3.13 KiB (4.75 KiB)
Row Confidence Table	1024 entries, 8 ways, 25 bits per entry: 9-bit row tag, 3-bit LRU, 8-bit confidence, 3-bit issue counter (max 5), 2-bit useful counter (max 4)	3.13 KiB
Page Occupancy Table	256 entries, 8 ways, 100 bits per entry: 36-bit 4 KiB page id, 64-bit page occupancy map	3.13 KiB
Bank-leveling Buffer	64 total entries / core (16 sub-buffers), 47 bits per entry: 42-bit block number, 3-bit cpy id, 1-bit engine-id, 1-bit pending flag	376 B
HSD Histogram	2 histograms, 64 entries each, 13 bits per entry: access count	(1.63 KiB)
HSD State Machine	3-bit state machine register, 13-bit epoch counter (2 B)	
HSD Stream Manager	32 streams, 106 bits per stream: 48-bit IP, 36-bit 4 KiB page id, 6-bit last-offset, 5-bit depth, 3-bit stride, 8-bit age	(424 B)
LLC	128 K lines, 16 KiB: log2(engines)-bit prefetch-engine id per block	(16 KiB)
ORAP		9.76 KiB
ORAP + HSD		29.42 KiB

TABLE IV: State Overhead of ORAP

ChampSim is modified to support prefetch promotion, a performance optimization where demands can mark prefetches they are waiting on for prioritization by the memory system. Additionally, ramulator2 utilizes an adaptive row policy and scheduler from prior work [22, 27]. Our system configuration is listed in Table III, which is modeled after recent Zen4 cores, including their 64 MiB 3D-integrated caches [59].

For evaluating energy results, we report normalized DRAM dynamic energy per instruction (DEPI) which serves as a unit of the energy efficiency of the system. Energies are obtained through ramulator2's energy model. Under an Adaptive Row Policy, we identify dynamic energy as energy expended over an idle system, including the energy to execute DRAM commands and keep banks active.

We evaluate ORAP on all workloads in the selected benchmark suites, with the exception of bc.kron, bc.urand, bfs.urand, sssp.urand, sssp.kron, sssp.twitter, sssp.web, and tc.urand from GAP which were excluded due to simulation infrastructure constraints. Every simpoint for each workload was simulated in single-core. For 8-core simulations, 73 mixes were randomly compiled from all simpoints.

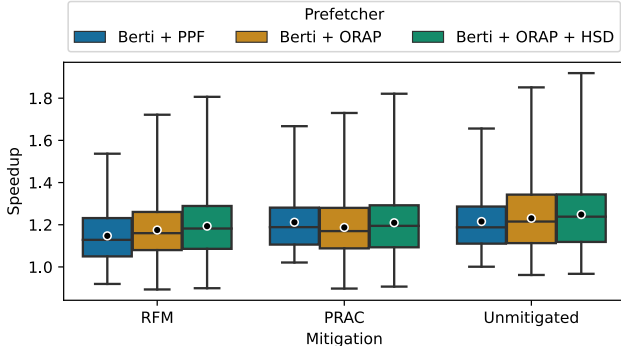


Fig. 15: Average multi-core speedup under different mitigations

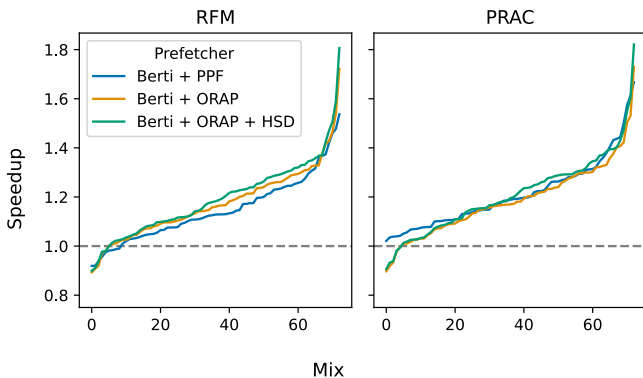


Fig. 16: Sorted speedups of mixes under RFM and PRAC mitigations

B. Results

1) *Storage Overheads*: Compared to the state-of-the-art Berti and PPF prefetching scheme, Berti + ORAP and Berti + ORAP + HSD reduce necessary state by 67.7% (9.76 KiB) and 22.7% (30.66 KiB) respectively. As shown in Table IV, ORAP requires relatively little state per core resulting in a small area overhead to the entire LLC (0.37%). The primary overhead of adding HSD comes from differentiating Next-Column and HSD prefetches, which requires an additional bit in each line of the cache.

2) *Multi-core Performance*: Multi-core speedup across all 73 mixes is provided in Figure 15, normalized to a non-prefetching system. The average mix speedup over Berti + PPF for Berti + ORAP + HSD was 4.6% in RFM systems, 3.3% speedup in unmitigated systems, and a 0.24% slowdown in PRAC systems. ORAP has both higher maximum and lower minimum speedups (indicated by the whiskers) than Berti + PPF. From Figure 16, it can be seen that ORAP is consistently better than Berti + PPF under RFM, yet struggles on the lowest-performing workloads under PRAC. As we will see, however, while ORAP performance under PRAC is slightly worse, it significantly reduces activation rates and energy consumption.

Berti + PPF saw a 6.8% and 0.35% slowdown for RFM and PRAC respectively, compared to the non-prefetching overheads of 5.1% and 0.15%. Interestingly, ORAP suffers a 5.48% and 3.88% slowdown over its unmitigated counterpart for RFM and PRAC. This suggests that while ORAP reduces the overhead of RFM mitigations, it is sensitive to the timing changes under PRAC. PRAC increases precharge times over baseline, meaning that rowbuffer conflicts come at greater penalties. Since ORAP increases the number of blocks fetched from an opened rowbuffer, the Adaptive Row Policy in the memory controller may learn to hold rowbuffers open longer, increasing the risk of conflicts and the total PRAC overhead. The recent work by Kim et al. [27] explores these PRAC interactions with row policies in more detail.

3) *DRAM Activation Rates and Dynamic Energy*: Figure 18 shows the multi-core activation rates (activations per thousand instructions) of Berti + PPF and ORAP normalized to a non-prefetching system. Compared to Berti + PPF’s activation rates, rates are reduced by 54.2% and 51.3% for Berti + ORAP and Berti + ORAP + HSD respectively. This reduction was the primary goal of ORAP’s design, but fails to achieve the loftier goals of reducing rates to below baseline. This suggests that further reduction in rates would require redesigns within ORAP or expanding the purview of the design into memory controller policy and address mappings.

We analyze the dynamic energy of the DRAM normalized to the baseline energy overhead of each mitigation. Generally, we find that dynamic energy is reduced over a non-prefetching system, with Berti + PPF showing a 5.34% reduction over baseline for an unmitigated system. For Berti + ORAP + HSD, energy is further reduced by 2.02% and 0.55% for RFM and unmitigated systems. The difference in dynamic energy is most drastic under PRAC mitigations. Since the rates of DRAM activations are substantially higher under Berti + PPF, so are the energy overheads associated with precharges. ORAP’s reduction in activation rates translates to significant energy reduction: 11.8%.

4) *Prefetch Usefulness and DRAM Bandwidth*: ORAP’s prefetching strategy is aggressive, and while it tries to preserve the usefulness of prefetches, it is designed to prefetch in a way that is counter to that goal. ORAP prefetches deeply into pages, so preserving usefulness is difficult. We find that ORAP as a replacement for PPF has lower overall usefulness, dropping from 57% to 47%. ORAP prefetches in the LLC, so space is abundant and small drops in usefulness are less impactful than if it were placing in the L2. ORAP avoids DRAM activations when issuing prefetches, so these prefetches consume relatively little energy and are not typically disruptive.

Compared to Berti + PPF, average bandwidth utilization rises from 31.4 GiB/s to 39.6 GiB/s across our mixes. At the same time, average DRAM latency rose from 281 cycles to 323 cycles. Figure 19 displays the distribution of different mixes across DRAM bandwidth and latency for Berti + PPF and Berti + ORAP + HSD. Note that for Berti + PPF as bandwidth utilization begins to increase DRAM latency rises sharply. However, Berti + ORAP + HSD’s latency rises

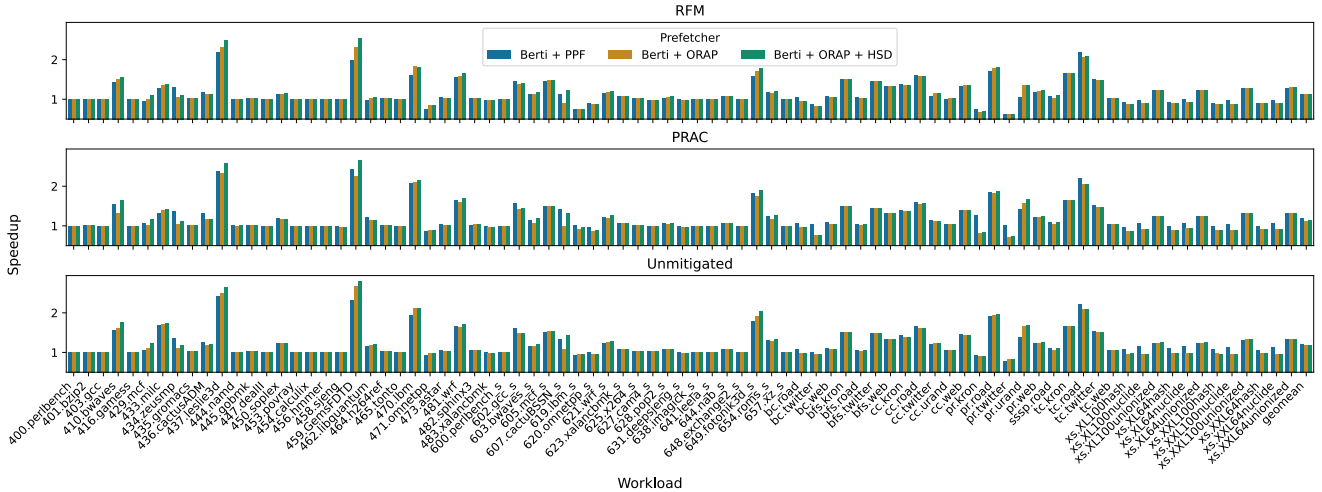


Fig. 17: Single-core speedup of ORAP vs. Berti + PPF

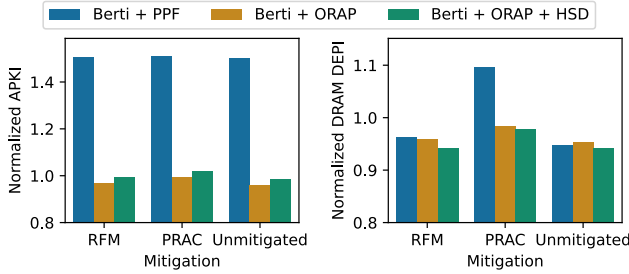


Fig. 18: DRAM activation rates (left) compared to DRAM dynamic energy (right)

gradually, and has a lower peak latency and higher peak bandwidth utilization than Berti + PPF. We attribute this to two complementary negative impacts of Berti + PPF's prefetching behavior. First, we noted that increased rowbuffer conflicts could cause performance loss in Section IV-B2. Although Berti + PPF is unlikely to cause rowbuffers to remain open for long times like ORAP, it is likely to access rowbuffers which are not open to the requested row. As a result, scheduling policies within the memory controller may choose to delay these packets to serve packets that will result in rowbuffer hits, which in turn limits Berti + PPF's ability to exploit DRAM bandwidth. The second cause for this behavior is the reduced latency of rowbuffer hits. Since ORAP requests multiple blocks from a single open rowbuffer, its packets always hit, and as a result are not only served quicker, but have an overall lower access latency. These combined behaviors mean that ORAP can utilize more DRAM bandwidth while having less overall impact on the performance of the memory system, conditioned on timings that minimize the disruption of long contiguous streams of rowbuffer hits.

5) *Single-core Performance*: The single-core performance of various prefetchers under RFM and PRAC mitigations can be seen in Figure 1. We further breakdown their performance

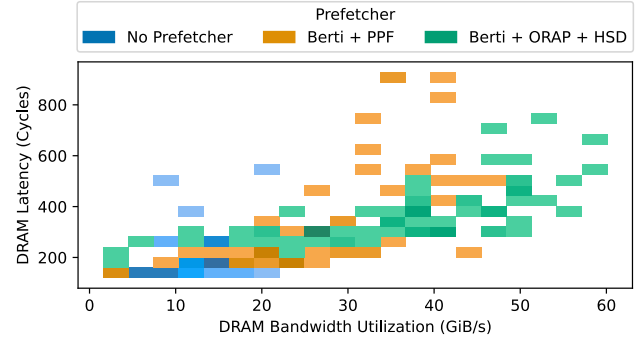


Fig. 19: Bandwidth consumption between ORAP and Berti + PPF under an RFM-mitigated system

across workloads for Berti + PPF, Berti + ORAP, and Berti + ORAP + HSD in Figure 17. Compared to a no-prefetching baseline, Berti + ORAP + HSD provides 12.8% geomean speedup and outperforms the state-of-the-art by 1.2% under RFM. In PRAC and unmitigated systems, ORAP incurs a 3.28% and 0.4% performance loss respectively. We find that ORAP outperforms Berti + PPF on many SPEC2006, SPEC2017, and GAP workloads. ORAP is consistently worse for many of the XSBench workloads, though this margin is significantly reduced under RFM mitigations.

V. CONCLUSION AND FUTURE WORK

ORAP offers considerable improvements over the current state-of-the-art in prefetching. ORAP outperforms the state-of-the-art, showing performance speedup of 4.6% in RFM-mitigated systems and reducing DRAM dynamic energy by 11.8% in PRAC-mitigated systems. ORAP uses 22.7% less state in its largest form, and overcomes the limitations of previous DRAM-aware prefetchers by the targeted prefetching of deep access streams and issuing requests out-of-order to

maximize rowbuffer hit rate and bank-level-parallelism. ORAP leverages large page sizes, large cache state, and modern memory systems to improve overall interactions between hardware prefetchers, caches, and DRAM to achieve significant performance improvement. While these contributions are considerable, more work can be done to improve this system. Other prefetchers may fare better alongside ORAP than HSD or Berti, and considerable improvements can still be made to ORAP’s overall prefetcher usefulness.

VI. ACKNOWLEDGEMENTS

Portions of this research were conducted with the advanced computing resources provided by Texas A&M High Performance Research Computing.

The authors acknowledge the support from the Purdue Center for a Secure Microelectronics Ecosystem [CSME#210205].

REFERENCES

[1] “Amd-v™ nested paging – white paper,” 2008. [Online]. Available: <https://www.cse.iitd.ac.in/~sbansal/csl862-virt/2010/readings/NPT-WP-1%201-final-TM.pdf>

[2] “Database tuning on linux os: Reference guide for amd epyc™ 7002 series processors,” 2019. [Online]. Available: https://www.amd.com/content/dam/amd/en/documents/epyc-technical-docs/tuning-guides/2019-amd-epyc-7002-tg-linux-databse-56783_1_0.pdf

[3] “Virtual memory support, armv4 and armv5,” 2025. [Online]. Available: <https://developer.arm.com/documentation/ddi0406/cb/Appendices/ARMv4-and-ARMv5-Differences/System-level-memory-model/Virtual-memory-support>

[4] M. Bakhshaliour, M. Shakerinava, P. Lotfi-Kamran, and H. Sarbazi-Azad, “Bingo spatial data prefetcher,” in *2019 IEEE International Symposium on High Performance Computer Architecture (HPCA)*, 2019, pp. 399–411.

[5] S. Beamer, K. Asanović, and D. Patterson, “The gap benchmark suite,” 2017. [Online]. Available: <https://arxiv.org/abs/1508.03619>

[6] E. Bhatia, G. Chacon, S. Pugsley, E. Teran, P. V. Gratz, and D. A. Jiménez, “Perceptron-based prefetch filtering,” in *2019 ACM/IEEE 46th Annual International Symposium on Computer Architecture (ISCA)*, 2019, pp. 1–13.

[7] M. Bruce, *Arm Neoverse V2 platform: Leadership Performance and Power Efficiency for NextGeneration Cloud Computing, ML and HPC Workloads*. IEEE, 2023.

[8] O. Canpolat, A. G. Yağlıkçı, G. F. Oliveira, A. Olgun, O. Ergin, and O. Mutlu, “Understanding the security benefits and overheads of emerging industry solutions to dram read disturbance,” 2024. [Online]. Available: <https://arxiv.org/abs/2406.19094>

[9] P. Frigo, E. Vannacci, H. Hassan, V. van der Veen, O. Mutlu, C. Giuffrida, H. Bos, and K. Razavi, “TRRespass: Exploiting the Many Sides of Target Row Refresh,” in *S&P*, May 2020, best Paper Award, Pwnie Award for Most Innovative Research, IEEE Micro Top Picks Honorable Mention, DCSR Paper Award. [Online]. Available: Paper=https://download.vusec.net/papers/trrespass_sp20.pdfSlides=https://download.vusec.net/slides/trrespass_sp20.pdfWeb=<https://www.vusec.net/projects/trrespassCode>=<https://github.com/vusec/trrespassPress>=<https://bit.ly/2UXWKJ4>

[10] J. Fu, J. Patel, and B. Janssens, “Stride directed prefetching in scalar processors,” in *[1992] Proceedings the 25th Annual International Symposium on Microarchitecture MICRO 25*, 1992, pp. 102–110.

[11] N. Gober, G. Chacon, L. Wang, P. V. Gratz, D. A. Jiménez, E. Teran, S. Pugsley, and J. Kim, “The championship simulator: Architectural simulation for education and competition,” 2022.

[12] B. Grayson, J. Rupley, G. Z. Zuraski, E. Quinnell, D. A. Jiménez, T. Nakra, P. Kitchin, R. Hensley, E. Brekelbaum, V. Sinha, and A. Ghiya, “Evolution of the samsung exynos cpu microarchitecture,” in *2020 ACM/IEEE 47th Annual International Symposium on Computer Architecture (ISCA)*, 2020, pp. 40–51.

[13] F. Guo, S. Kim, Y. Baskakov, and I. Banerjee, “Proactively breaking large pages to improve memory overcommitment performance in vmware esxi,” *SIGPLAN Not.*, vol. 50, no. 7, p. 39–51, Mar. 2015. [Online]. Available: <https://doi.org/10.1145/2817817.2731187>

[14] I. Hur and C. Lin, “Memory prefetching using adaptive stream detection,” in *2006 39th Annual IEEE/ACM International Symposium on Microarchitecture (MICRO’06)*, 2006, pp. 397–408.

[15] “Intel® 64 and ia-32 architectures software developer manuals,” 2025. [Online]. Available: <https://www.intel.com/content/www/us/en/developer/articles/technical/intel-sdm.html>

[16] Y. Ishii, M. Inaba, and K. Hiraki, “Access map pattern matching for data cache prefetch,” in *Proceedings of the 23rd International Conference on Supercomputing*, ser. ICS ’09. New York, NY, USA: Association for Computing Machinery, 2009, p. 499–500. [Online]. Available: <https://doi.org/10.1145/1542275.1542349>

[17] —, “Unified memory optimizing architecture: memory subsystem control with a unified predictor,” in *Proceedings of the 26th ACM International Conference on Supercomputing*, ser. ICS ’12. New York, NY, USA: Association for Computing Machinery, 2012, p. 267–278. [Online]. Available: <https://doi.org/10.1145/2304576.2304614>

[18] P. Jattke, M. Wipfli, F. Solt, M. Marazzi, M. Bölskei, and K. Razavi, “ZenHammer: Rowhammer attacks on AMD zen-based platforms,” in *33rd USENIX Security Symposium (USENIX Security 24)*. Philadelphia, PA: USENIX Association, Aug. 2024, pp. 1615–1633. [Online]. Available: <https://www.usenix.org/conference/usenixsecurity24/presentation/jattke>

[19] JEDEC, “Jesd79-5: Ddr5 sdram standard,” 2020.

[20] —, “Jesd79-5c: Ddr5 sdram standard,” 2024.

[21] I. Kang, W. Wang, J. Kim, S. van Schaik, Y. Tobah,

D. Genkin, A. Kwong, and Y. Yarom, “Sledgehammer: amplifying rowhammer via bank-level parallelism,” in *Proceedings of the 33rd USENIX Conference on Security Symposium*, ser. SEC ’24. USA: USENIX Association, 2024.

[22] D. Kaseridis, J. Stuecheli, and L. K. John, “Minimalist open-page: a dram page-mode scheduling policy for the many-core era,” in *Proceedings of the 44th Annual IEEE/ACM International Symposium on Microarchitecture*, ser. MICRO-44. New York, NY, USA: Association for Computing Machinery, 2011, p. 24–35. [Online]. Available: <https://doi.org/10.1145/2155620.2155624>

[23] J. S. Kim, M. Patel, A. G. Yağlıkçı, H. Hassan, R. Azizi, L. Orosa, and O. Mutlu, “Revisiting rowhammer: an experimental analysis of modern dram devices and mitigation techniques,” in *Proceedings of the ACM/IEEE 47th Annual International Symposium on Computer Architecture*, ser. ISCA ’20. IEEE Press, 2020, p. 638–651. [Online]. Available: <https://doi.org/10.1109/ISCA45697.2020.00059>

[24] J. S. Kim, M. Patel, A. G. Yağlıkçı, H. Hassan, R. Azizi, L. Orosa, and O. Mutlu, “Revisiting rowhammer: An experimental analysis of modern dram devices and mitigation techniques,” in *2020 ACM/IEEE 47th Annual International Symposium on Computer Architecture (ISCA)*, 2020, pp. 638–651.

[25] J. Kim, S. H. Pugsley, P. V. Gratz, A. N. Reddy, C. Wilkerson, and Z. Chishti, “Path confidence based lookahead prefetching,” in *2016 49th Annual IEEE/ACM International Symposium on Microarchitecture (MICRO)*, 2016, pp. 1–12.

[26] J. Kim, E. Teran, P. V. Gratz, D. A. Jiménez, S. H. Pugsley, and C. Wilkerson, “Kill the program counter: Reconstructing program behavior in the processor cache hierarchy,” in *Proceedings of the Twenty-Second International Conference on Architectural Support for Programming Languages and Operating Systems*, ser. ASPLOS ’17. New York, NY, USA: Association for Computing Machinery, 2017, p. 737–749. [Online]. Available: <https://doi.org/10.1145/3037697.3037701>

[27] J. Kim, S. Baek, M. Wi, H. Nam, M. J. Kim, S. Lee, K. Sohn, and J. H. Ahn, “Per-row activation counting on real hardware: Demystifying performance overheads,” *IEEE Computer Architecture Letters*, vol. 24, no. 2, p. 217–220, Jul. 2025. [Online]. Available: <http://dx.doi.org/10.1109/LCA.2025.3587293>

[28] M. J. Kim, J. Park, Y. Park, W. Doh, N. Kim, T. J. Ham, J. W. Lee, and J. H. Ahn, “Mithril: Cooperative Row Hammer Protection on Commodity DRAM Leveraging Managed Refresh,” in *2022 IEEE International Symposium on High-Performance Computer Architecture (HPCA)*. Los Alamitos, CA, USA: IEEE Computer Society, Apr. 2022, pp. 1156–1169. [Online]. Available: <https://doi.ieeecomputersociety.org/10.1109/HPCA53966.2022.00088>

[29] Y. Kim, R. Daly, J. Kim, C. Fallin, J. H. Lee, D. Lee, C. Wilkerson, K. Lai, and O. Mutlu, “Flipping bits in memory without accessing them: an experimental study of dram disturbance errors,” in *Proceeding of the 41st Annual International Symposium on Computer Architecture*, ser. ISCA ’14. IEEE Press, 2014, p. 361–372.

[30] —, “Flipping bits in memory without accessing them: an experimental study of dram disturbance errors,” in *Proceeding of the 41st Annual International Symposium on Computer Architecture*, ser. ISCA ’14. IEEE Press, 2014, p. 361–372.

[31] A. Kwong, D. Genkin, D. Gruss, and Y. Yarom, “Ramble: Reading bits in memory without accessing them,” in *2020 IEEE Symposium on Security and Privacy (SP)*, 2020, pp. 695–711.

[32] C. J. Lee, V. Narasiman, O. Mutlu, and Y. N. Patt, “Improving memory bank-level parallelism in the presence of prefetching,” in *2009 42nd Annual IEEE/ACM International Symposium on Microarchitecture (MICRO)*, 2009, pp. 327–336.

[33] H. Luo, A. Olgun, A. G. Yağlıkçı, Y. C. Tuğrul, S. Rhyner, M. B. Cavlak, J. Lindegger, M. Sadrosadati, and O. Mutlu, “Rowpress: Amplifying read disturbance in modern dram chips,” in *Proceedings of the 50th Annual International Symposium on Computer Architecture*, ser. ISCA ’23. New York, NY, USA: Association for Computing Machinery, 2023. [Online]. Available: <https://doi.org/10.1145/3579371.3589063>

[34] H. Luo, Y. C. Tuğrul, F. N. Bostancı, A. Olgun, A. G. Yağlıkçı, and O. Mutlu, “Ramulator 2.0: A modern, modular, and extensible dram simulator,” 2023. [Online]. Available: <https://arxiv.org/abs/2308.11030>

[35] “Transparent huge pages,” 2011. [Online]. Available: <http://lwn.net/Articles/423584/>

[36] “Kernel address space layout randomization,” 2013. [Online]. Available: <https://lwn.net/Articles/569635/>

[37] P. Michaud, “Best-offset hardware prefetching,” in *2016 IEEE International Symposium on High Performance Computer Architecture (HPCA)*, 2016, pp. 469–480.

[38] O. Mutlu, “The rowhammer problem and other issues we may face as memory becomes denser,” in *Design, Automation and Test in Europe Conference and Exhibition (DATE)*, 2017, 2017, pp. 1116–1121.

[39] O. Mutlu and J. S. Kim, “Rowhammer: A retrospective,” *Trans. Comp.-Aided Des. Integ. Cir. Sys.*, vol. 39, no. 8, p. 1555–1571, Aug. 2020. [Online]. Available: <https://doi.org/10.1109/TCAD.2019.2915318>

[40] P. J. Nair, D.-H. Kim, and M. K. Qureshi, “Archshield: architectural framework for assisting dram scaling by tolerating high error rates,” *SIGARCH Comput. Archit. News*, vol. 41, no. 3, p. 72–83, Jun. 2013. [Online]. Available: <https://doi.org/10.1145/2508148.2485929>

[41] J. Navarro, S. Iyer, and A. Cox, “Practical, transparent operating system support for superpages,” in *5th Symposium on Operating Systems Design and Implementation (OSDI 02)*. Boston, MA:

USENIX Association, Dec. 2002. [Online]. Available: <https://www.usenix.org/conference/osdi-02/practical-transparent-operating-system-support-superpages>

[42] A. Navarro-Torres, B. Panda, J. Alastruey-Benedé, P. Ibáñez, V. Viñals-Yúfera, and A. Ros, “Berti: an accurate local-delta data prefetcher,” in *2022 55th IEEE/ACM International Symposium on Microarchitecture (MICRO)*, 2022, pp. 975–991.

[43] R. Nazaraliyev, S. Ganjisaffar, N. Nazaraliyev, and N. Abu-Ghazaleh, “Practical: Subarray-level counter update and bank-level recovery isolation for efficient prac rowhammer mitigation,” 2025. [Online]. Available: <https://arxiv.org/abs/2507.18581>

[44] S. Pakalapati and B. Panda, “Bouquet of instruction pointers: Instruction pointer classifier-based spatial hardware prefetching,” in *2020 ACM/IEEE 47th Annual International Symposium on Computer Architecture (ISCA)*, 2020, pp. 118–131.

[45] Y. Park, W. Kwon, E. Lee, T. J. Ham, J. Ho Ahn, and J. W. Lee, “Graphene: Strong yet lightweight row hammer protection,” in *2020 53rd Annual IEEE/ACM International Symposium on Microarchitecture (MICRO)*, 2020, pp. 1–13.

[46] E. Perelman, G. Hamerly, M. Van Biesbrouck, T. Sherwood, and B. Calder, “Using simpoint for accurate and efficient simulation,” in *Proceedings of the 2003 ACM SIGMETRICS International Conference on Measurement and Modeling of Computer Systems*, ser. SIGMETRICS ’03. New York, NY, USA: Association for Computing Machinery, 2003, p. 318–319. [Online]. Available: <https://doi.org/10.1145/781027.781076>

[47] M. Qureshi, “Autofrm: Scaling low-cost in-dram trackers to ultra-low rowhammer thresholds,” in *2025 IEEE International Symposium on High Performance Computer Architecture (HPCA)*, 2025, pp. 991–1004.

[48] M. Qureshi and S. Qazi, “Moat: Securely mitigating rowhammer with per-row activation counters,” in *Proceedings of the 30th ACM International Conference on Architectural Support for Programming Languages and Operating Systems, Volume 1*, ser. ASPLOS ’25. New York, NY, USA: Association for Computing Machinery, 2025, p. 698–714. [Online]. Available: <https://doi.org/10.1145/3669940.3707278>

[49] M. Qureshi, S. Qazi, and A. Jaleel, “Mint: Securely mitigating rowhammer with a minimalist in-dram tracker,” in *Proceedings of the 2024 57th IEEE/ACM International Symposium on Microarchitecture*, ser. MICRO ’24. IEEE Press, 2024, p. 899–914. [Online]. Available: <https://doi.org/10.1109/MICRO61859.2024.00071>

[50] M. Qureshi, A. Rohan, G. Saileshwar, and P. J. Nair, “Hydra: enabling low-overhead mitigation of rowhammer at ultra-low thresholds via hybrid tracking,” in *Proceedings of the 49th Annual International Symposium on Computer Architecture*, ser. ISCA ’22. New York, NY, USA: Association for Computing Machinery, 2022, p. 699–710. [Online]. Available: <https://doi.org/10.1145/3470496.3527421>

[51] V. S. S. Ram, A. Panwar, and A. Basu, “Trident: Harnessing architectural resources for all page sizes in x86 processors,” in *MICRO-54: 54th Annual IEEE/ACM International Symposium on Microarchitecture*, ser. MICRO ’21. New York, NY, USA: Association for Computing Machinery, 2021, p. 1106–1120. [Online]. Available: <https://doi.org/10.1145/3466752.3480062>

[52] G. Saileshwar, B. Wang, M. Qureshi, and P. J. Nair, “Randomized row-swap: mitigating row hammer by breaking spatial correlation between aggressor and victim rows,” in *Proceedings of the 27th ACM International Conference on Architectural Support for Programming Languages and Operating Systems*, ser. ASPLOS ’22. New York, NY, USA: Association for Computing Machinery, 2022, p. 1056–1069. [Online]. Available: <https://doi.org/10.1145/3503222.3507716>

[53] A. Saxena, S. Mathur, and M. Qureshi, “Rubix: Reducing the overhead of secure rowhammer mitigations via randomized line-to-row mapping,” in *Proceedings of the 29th ACM International Conference on Architectural Support for Programming Languages and Operating Systems, Volume 2*, ser. ASPLOS ’24. New York, NY, USA: Association for Computing Machinery, 2024, p. 1014–1028. [Online]. Available: <https://doi.org/10.1145/3620665.3640404>

[54] A. Saxena, G. Saileshwar, P. J. Nair, and M. Qureshi, “Aqua: Scalable rowhammer mitigation by quarantining aggressor rows at runtime,” in *2022 55th IEEE/ACM International Symposium on Microarchitecture (MICRO)*, 2022, pp. 108–123.

[55] “Spec cpu2006,” 2025. [Online]. Available: <https://www.spec.org/cpu2006>

[56] “Spec cpu2017,” 2025. [Online]. Available: <https://www.spec.org/cpu2017>

[57] J. Tramm, A. Siegel, T. Islam, and M. Schulz, “Xsbench - the development and verification of a performance abstraction for monte carlo reactor analysis,” 09 2014.

[58] G. Vavouliotis, G. Chacon, L. Alvarez, P. V. Gratz, D. A. Jiménez, and M. Casas, “Page size aware cache prefetching,” in *2022 55th IEEE/ACM International Symposium on Microarchitecture (MICRO)*, 2022, pp. 956–974.

[59] “Ryzen 7 7800x3d - amd.” [Online]. Available: https://en.wikichip.org/wiki/amd/ryzen_7/7800x3d

[60] J. Woo, J. Qu, G. Saileshwar, and P. J. Nair, “When mitigations backfire: Timing channel attacks and defense for prac-based rowhammer mitigations,” in *Proceedings of the 52nd Annual International Symposium on Computer Architecture*, ser. ISCA ’25. New York, NY, USA: Association for Computing Machinery, 2025, p. 739–756. [Online]. Available: <https://doi.org/10.1145/3695053.3731007>

[61] C.-J. Wu, A. Jaleel, W. Hasenplaugh, M. Martonosi, S. C. Steely, and J. Emer, “Ship: Signature-based hit predictor for high performance caching,” in *2011 44th Annual IEEE/ACM International Symposium on Microarchitec-*

ture (MICRO), 2011, pp. 430–441.

- [62] C.-J. Wu, A. Jaleel, M. Martonosi, S. C. Steely, and J. Emer, “Pacman: prefetch-aware cache management for high performance caching,” in *Proceedings of the 44th Annual IEEE/ACM International Symposium on Microarchitecture*, ser. MICRO-44. New York, NY, USA: Association for Computing Machinery, 2011, p. 442–453. [Online]. Available: <https://doi.org/10.1145/2155620.2155672>
- [63] L. Xu, R. Yu, L. Wang, and W. Liu, “Memway: in-memorywaylaying acceleration for practical rowhammer attacks against binaries,” *Tsinghua Science and Technology*, vol. 24, no. 5, pp. 535–545, 2019.
- [64] A. G. Yağlıkçı, M. Patel, J. S. Kim, R. Azizi, A. Olgun, L. Orosa, H. Hassan, J. Park, K. Kanellopoulos, T. Shahroodi, S. Ghose, and O. Mutlu, “Blockhammer: Preventing rowhammer at low cost by blacklisting rapidly-accessed dram rows,” in *2021 IEEE International Symposium on High-Performance Computer Architecture (HPCA)*, 2021, pp. 345–358.